Calibration and Modelling of the Semmes-Weinstein Monofilament for Diabetic Foot Management

Pedro Castro-Martins , Luis Coelho * , R.D.S.G. Campilho

Posted Date: 24 April 2024

doi: 10.20944/preprints202404.1560.v1

Keywords: Diabetic Foot; Monofilament; Metrological Verification; Buckling Force

 doi:10.20944/preprints202404.1560.v1

Article

Calibration and Modelling of the Semmes-Weinstein Monofilament for Diabetic Foot Management

Pedro Castro-Martins [1,2,†], Luís Pinto-Coelho [1,3,*,†] and Raul D. S. G. Campilho [4,5,†]

[1] CIETI, School of Engineering, Polytechnic of Porto, Portugal; pmdcm@isep.ipp.pt (PCM)
[2] Faculty of Engineering, University of Porto, Portugal
[3] INESC-TEC, Centre for Robotics in Industry and Intelligent Systems, Porto, Portugal
[4] Mechanical Engineering Department, School of Engineering, Polytechnic of Porto, Portugal; rds@isep.ipp.pt
[5] INEGI, Institute of Science and Innovation in Mechanical and Industrial Engineering, Porto, Portugal
* Correspondence: lfc@isep.ipp.pt; Instituto Superior de Engenharia do Porto, Rua Dr. António Bernardino de Almeida 431, 4249-015 Porto, Portugal
† These authors contributed equally to this work.

Abstract: Diabetic foot is a serious complication that poses significant risks for diabetic people. The resulting reduction in protective sensitivity in the plantar region requires early detection to prevent the imminent ulceration and amputation. The primary method employed for evaluating this sensitivity loss is the 10 gf Semmes-Weinstein monofilament test, commonly used as a first-line procedure. However, the lack of calibration in existing devices often introduces decision errors due to unreliable feedback. In this paper, a new equipment designed to address these limitations and enhance the assessment of the sensitivity loss using the 10 gf monofilament is introduced. The proposed system automates metrological verification and evaluation processes, ensuring accurate and reliable results. Furthermore, it simulates the practitioner's procedure, serving both as a valuable training tool and a means to provide force-feedback information. An analytical model of the monofilament buckling and deflection is also presented. The obtained results showed that the tested monofilaments had a very high error compared to the 10 gf declared by the manufacturers. It is aimed, by introducing this advanced equipment, to improve the precision and reliability of assessing the sensitivity loss. The integration of automated verification, simulation capabilities, and precise measurements shows great promise for diabetic patients, reducing the likelihood of adverse outcomes such as ulceration and amputation.

Keywords: diabetic foot; monofilament; metrological verification; buckling force

1. Introduction

Diabetes is an incurable chronic disease that is growing exponentially all over the world, especially in most developed countries. It presents several complications, but when associated with other comorbidities, serious problems arise for the patient, as is the case of the diabetic foot. This pathology results in complications in the lower limbs, namely in the plantar region, whose evolution can have devastating effects and with a high probability of compromising part of the affected limb [1]. As a preventive measure, tests are periodically carried out to assess the loss of skin sensitivity to pressure on the foot, with the objective of identifying situations of risk of imminent injury. The 10 gf Semmes-Weinstein monofilament (SWM) test is the most used first-line instrument in the assessment of loss of protective sensitivity in the diabetic foot (see Figure 1), with international recommendations for its widespread use [1–3]. This instrument is made up of a thin nylon filament (or other flexible plastic material, sometimes unknown) and its application technique basically consists of promoting a touch with the monofilament on the skin, in a perpendicular orientation, until it performs a slight curvature. At this point, a value of equal strength to what the instrument manufacturer declares will have been applied [4].

 doi:10.20944/preprints202404.1560.v1

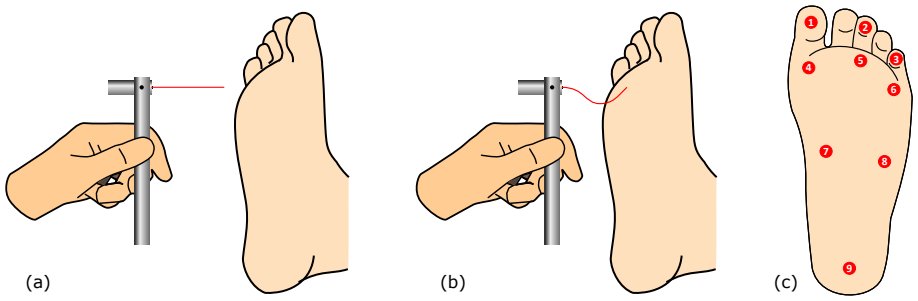

Figure 1. Plantar sensitivity assessment using the monofilament, showing: (**a**) the approaching stage; (**b**) the contact stage, with visible buckling; and (**c**) the related evaluation points, for the left foot.

This assessment is most often performed manually, by an experienced health professional, but it can also be performed automatically, using a collaborative robot [5,6]. The SWM only provides a binary qualitative assessment, as the health professional cannot obtain a numerical value as a result of the test. This prevents an objective comparison between the various screening tests, when, in the case of non-sensitivity feedback, the patient will be classified as at risk [2,7]. Another factor to be taken into account is the unknown measurement error that may be associated with the use of the SWM as decision making support device, even when the literature indicates the need to carry out quantitative assessments of the degree of loss of sensitivity in the diabetic foot. Thus, some authors have been presenting evidences that indicate a clear distrust regarding the real buckling force value that a SWM imposes on a patient's skin during a sensitivity screening test [8–11].

One issue to consider is that the compressive force of the monofilament tends to decrease with the number of successive uses, resulting in a significant change in its initial elastic characteristics. This condition may introduce significant errors in the assessments performed on a given patient after repeated usage, moreover the number of uses from which the monofilament begins to induce a significant error is effectively unknown [9]. Other variables to consider are the temperature and relative moisture of the air, that can significantly influence the compression force, dimensions and consequent deformation of the SWM. Tests on laboratory balances in different environments under different controlled temperature and moisture conditions showed that the force exerted by the monofilament progressively decreased up to approximately 40%, with temperature and moisture conditions ranging up to 37 °C and 80%, respectively [12].

In addition, if a nylon product absorbs moisture, dimensional changes will occur with increasing moisture content [13]. However, these variations are small in controlled environments, as happens in most healthcare facilities, making this a negligible effect for the current study.

SWM performance is still rather unexplored, despite its impact on medical decisions, however, this technique is widely used because it is simple and practical. It is routinely applied in periodic observations of the diabetic foot, used to select diabetics who still have protective sensitivity from those who do not [1,2,4,14]. However, there are guidelines that warn that the health professional should be aware of the possible loss of flexion strength of the monofilament, which may lead to the application of an inconstant force and different from that initially indicated by the manufacturer [14]. This reveals the need for health professionals to have equipment available to help them assess whether their monofilament is operating within the recommended strength ranges for diabetic foot screening and for all their clinical practice where this instrument can be used.

In this paper, the modeling of the monofilament behaviour under the plantar sensitivity test conditions is firstly presented. This allows to understand what are the critical parameters to observe during usage and during the devices' calibration. Then the thoroughly presentation of a new equipment is performed, extending a previous version [15], that is designed to evaluate the SWM in terms of its real compression force and, with this, to provide information to the health professional about the force range of their diagnostic instruments. This aims to improve the methodology for evaluating loss of sensitivity using the 10 gf SWM or other measurement points. This new equipment automates

 doi:10.20944/preprints202404.1560.v1

metrological verification and evaluation processes, ensuring accurate and reliable results. Furthermore, it simulates the practitioner's procedure, serving both as a valuable training tool and as a means of providing force feedback information from the SWM used. The calibration equipment is then used to test some devices whose properties are also explored using the analytical models. The obtained results are presented and widely discussed. Finally, the main aspects of the study are highlighted as well as envisioned future work.

2. Modeling the Monofilament

When performing the diabetic foot plantar sensitivity test using a monofilament, it is recommended to use monofilaments with specific characteristics to ensure consistent and standardized results. The SWM test is commonly used for this purpose, and it is commercially available in a set of distinct target force values with specific characteristics. These devices consist of nylon filaments that can have different diameters and lengths to apply a specific force to the skin when they are pressed and buckling. Usually referred to in grams by the medical community, the most commonly used target levels in the SWM test include 0.07 g, 0.16 g, 0.4 g, 0.6 g, 1 g, 2 g, 4 g, 10 g, and 300 g [16,17]. These target levels allow the evaluation of different levels of tactile sensitivity, with a 10 g monofilament being recommended for the evaluation of the diabetic foot [2,18].

Each monofilament is usually labeled with a number (during manufacturing) representing the force required to buckling it. These numbers range from 1.65 to 6.65 (evaluator size, a dimensionless scale) and indicate different standardized pressure values to be applied. The higher the number, the greater the force required to buckling the monofilament and therefore the greater the pressure exerted on the skin. For example, the evaluator size of 5.07 concerns a 10 g monofilament and, as such, the manufacturer states that a force of 10 gf is required for its buckling [16]. If this monofilament is applied to a specific point on the foot and the patient cannot feel the pressure, this may indicate a loss of sensitivity in that region [2,18].

2.1. Material

The monofilament is generally described as being made of nylon, which is generic designation for a family of synthetic polymers composed of polyamides. To specifically understand how the material behaves mechanically during operation, and in the context of use, it is necessary to have particular knowledge about it.

Concerning the material's properties, the most relevant to consider is the Young's Modulus. This property represents the stiffness of the nylon fiber, and it affects its resistance to buckling, with a higher Young's modulus indicating greater stiffness hence resisting buckling. The Yield stress and the Poisson's ratio can also be considered. These represent the ability to withstand deformation before experiencing permanent damage or failure and a measure of the material's lateral contraction when subjected to axial loading, respectively.

Extruded Nylon 6.6 (extruded polyamide 6.6) is the most common type and it is known for its high strength, stiffness, and excellent resistance to wear. However, it can be affected by moisture absorption, causing slight changes in its mechanical properties, including the Young's modulus. Nylon 6, an alternative, also widely used, has good mechanical strength, toughness, and abrasion resistance, being generally less affected by humidity compared to other types of nylon. Humidity absorption by nylon fibers can cause changes in the materials ability to resist compression or deflection. The relationship between humidity and the Young's modulus can be described using an empirical equation [19]:

$$E(H) = E_0 \cdot (1 - \beta \cdot (H - H_0)) \tag{1}$$

where $E(H)$ is the Young's modulus at humidity H, E_0 is the reference Young's modulus at a reference humidity H_0, and β is the humidity coefficient. The humidity coefficient (β) represents the rate at which the Young's modulus changes with humidity, and is typically provided by the material manufacturer,

 doi:10.20944/preprints202404.1560.v1

varying for different types of nylon. Humidity acts as a plasticizer in nylon and therefore reduces strength and stiffness properties but increases elongation and toughness. In general, as humidity content rises, significant increases occur in impact strength and other energy absorbing characteristics of the material.

The Young's modulus of a material usually decreases as temperature increases. This inverse relationship can be modeled using the following equation:

$$E(T) = E_0 \cdot (1 - \alpha \cdot (T - T_0)) \tag{2}$$

where: $E(T)$ is the Young's modulus at temperature T, E_0 is the reference Young's modulus at a reference temperature T_0, and α is the temperature coefficient of the material. The temperature coefficient (α) represents the rate at which the Young's modulus changes with temperature. Like humidity, it can vary for different types of nylon and is typically provided by the material manufacturer.

Besides material factors, geometry also plays a role. Length and diameter, or more specifically the length-to-diameter ratio of the fiber, is a critical geometric factor affecting buckling behavior. Longer fibers or fibers with smaller diameters are more prone to buckling. In addition, imperfections such as bends, eccentricities, or deviations from a perfect straight form, can amplify the tendency for buckling. Imperfections act as localized stress concentrations and can initiate buckling at lower loads. Imperfections can be a result of the manufacturing process but also a consequence of the monofilament misuse (for example when objects inadvertently cause permanent plastic deformations due to placing the monofilament device in a clothing pocket exposed to keys, a pen, or others). The boundary conditions imposed on the fiber ends can also significantly influence buckling [20]. In most cases, a fixed at one edge and pinned at the other (fixed-pinned) coupling is considered, but different skin stiffness can alter this behaviour leading to variations in buckling modes and critical buckling loads.

Finally, the loading conditions must also be taken into account. The magnitude and direction of the applied compressive load directly influence the buckling behavior with higher compressive loads increasing the risk of buckling. The rate at which the load is applied can also affect buckling behavior. Rapid loading or dynamic loading conditions may lead to different buckling responses compared to static loading [21].

It is important to note that the mentioned variables are interconnected, and their combined effects need to be considered in evaluating column buckling in a nylon fiber. Analytical methods, such as Euler's buckling theory or finite element analysis, can be employed to assess the influence of these variables, and predict both the critical buckling load and mode of failure for a specific nylon fiber column. Experimental testing can also provide valuable insights into the buckling behavior by considering these variables in a real-world scenario. In Table 1 a summary of which material characteristics can affect the monofilaments measurement performance is presented.

Table 1. Summary of factors that impact the monofilament behaviour.

Material	**Geometry**	**Loading Conditions**	**Environment**
Young's Modulus	Length and diameter	Compressive load	Temperature
Yield stress	End conditions	Load distribution	Moisture
Poisson's ratio	Imperfections	Loading rate	

2.2. Buckling

In practice, it is observed that 10 gf monofilaments are commercially available with a wide range of diameters and small variations in length. Most of the time, no information is given about the material from which it is produced. These characteristics can strongly impact the behavior of the monofilament when in operation, as will be shown in the following sections of this study.

 doi:10.20944/preprints202404.1560.v1

The buckling equation [22], also known as Euler's buckling equation, allows to estimate the force that leads to the initial buckling. It is given by:

$$F_c = \frac{\pi^2 \cdot E \cdot I}{L_e^2} \tag{3}$$

where F_c is the critical buckling force, E is the Young's modulus of the material, I is the 2^{nd} moment of inertia of the cross-sectional area, and L_e is the effective length of the filament. The effective length is calculated as $L_e = k \cdot L$ where k is defined taking into account the boundary conditions and L is the real length of the monofilament. The end near the handle of the monofilament will always be clamped while for the free end two possibilities can be considered. The first case will correspond to the most common situation where the point of contact with the skin has no slippage and which, due to the small diameter of the filament, can be considered as a hinged/pinned connection. When the skin surface at the contact point does not guarantee sufficient friction (due to oil, dryness, sweat dirt or other factors) then there will be a hinged connection with sliding. For the clamped-pinned case a theoretical $k = 0.7$ was defined, and for the clamped-(pinned and sliding) case $k = 2.0$ is the reference (clamped means rotation and translation fixed, pinned and sliding means rotation and translation free) [23].

To calculate the 2^{nd} moment of inertia (I) for a circular cross-section area, the following formula can be used:

$$I = \frac{\pi \cdot d^4}{64} \tag{4}$$

where d is the diameter of the filament.

Hence, defining the monofilament material, length and diameter allows us to estimate it critical buckling force. On the other hand, if the critical force is known, as well as the geometrical dimensions, then the Young's modulus for an unknown material can be estimated.

2.3. Deflection

During the evaluation of plantar sensitivity, the monofilament is positioned horizontally to move perpendicularly toward the patients foot. In this position, the nylon filament behaves like a cantilever beam subjected to distributed load, corresponding to its own weight, that will cause the deflection of the free extremity.

When a beam is not flexed or deflected, the applied load is mainly an axial load, meaning a force that acts along the longitudinal axis of the beam. The material of the beam is more efficient in supporting this type of load, as it is designed to resist compression and tension forces along its length. In this case, the load is transmitted directly to the supporting base, making the structure more stable and resistant.

On the other hand, when a beam is bent or flexed, it encounters extra forces known as bending moment and shear. This bending action causes the particles within the beam's material to move relative to each other, creating internal stresses. These internal stresses, if excessive or repeated, have the potential to weaken the structure. Bending moment is a specific type of force during this bending process, which includes both a bending force (trying to bend the beam) and torque (a twisting force). Over time, these combined forces from bending moment can lead to deformation and, ultimately, material failure. In simpler terms, when a beam bends, it experiences forces that can strain its material and gradually compromise its strength and shape. Additionally, shear, which is a cutting force perpendicular to the axis of the beam, can also affect the load-carrying capacity of the structure.

In this context, let us estimate the deflexion of the monofilament due to its weight. Considering a linear elastic deformation and a small deflection ($< 1/10$ of span), the displacement of the monofilament free extremity can be calculated from the general elastic equation [23]:

$$\frac{d^2y(x)}{dx^2} = \frac{M}{E \cdot I} \tag{5}$$

 doi:10.20944/preprints202404.1560.v1

where the x axis is defined along the length L of the monofilament, M is the bending momentum, E is the Young's modulus and I is the moment of inertia (Equation 4). The monofilament weight is given by:

$$w = V \cdot \rho \cdot g \tag{6}$$

where V is the volume of the monofilament, ρ the material's density and g the gravity. In the present case, the load is distributed along the monofilament and it can be expressed as $q = w/L$. In these conditions the monofilament elastic deflection in the free extremity $y(L) = \delta$ can be written as:

$$\delta = \frac{w \cdot L^4}{8 \cdot E \cdot I} \tag{7}$$

3. Monofilament Calibration Equipment

Medical device calibration holds significant importance within the healthcare industry for several compelling reasons. Firstly, calibration ensures the provision of accurate and reliable measurements by medical devices. This precision is paramount for diagnosing medical conditions, determining suitable treatment options, and effectively monitoring patient health. By establishing consistency and accuracy in readings, calibration contributes to the overall quality of healthcare delivery. Secondly, the major concern of patient safety is intricately linked to medical device calibration. An incorrectly calibrated device can lead to erroneous readings, potentially resulting in misdiagnosis, inappropriate treatment, or patient harm. Regular calibration practices serve as a crucial mechanism to identify and rectify any deviations or inaccuracies, thus minimizing the risk of adverse events and fostering patient well-being [24]. Moreover, regulatory standards and guidelines compliance is of utmost importance in the healthcare domain. Calibration is an indispensable component in meeting these requirements, as regulatory bodies, such as the Food and Drug Administration (FDA), often mandate regular calibration of medical devices to ensure both patient safety and device performance. Failure to comply with these regulations can result in severe consequences such as penalties, legal ramifications, and reputational damage for healthcare institutions [25].

Calibration serves as an integral part of quality control programs, ensuring that medical devices consistently adhere to established standards and specifications. By systematically calibrating devices at appropriate intervals, healthcare organizations can promptly identify and rectify any deviations or discrepancies in device performance. This proactive approach significantly contributes to maintaining the overall quality and reliability of diagnostic and therapeutic procedures, thereby fortifying the foundations of healthcare provision. In addition, calibration plays a pivotal role in preserving data integrity within healthcare settings. Numerous medical devices are seamlessly integrated with electronic health records (EHR) systems or employed for clinical research purposes. Calibration practices ensure the accuracy and reliability of the data generated by these devices, thereby bolstering the credibility of data analysis, research outcomes, and evidence-based decision-making within the medical community [26].

Another notable aspect lies in the extended lifespan and enhanced performance of medical devices due to regular calibration. By effectively detecting and rectifying any inaccuracies or signs of wear and tear, calibration mitigates the risk of premature device failures. Consequently, this practice reduces equipment downtime, minimizes repair costs, and optimizes operational efficiency within healthcare facilities, facilitating seamless healthcare delivery [26,27].

Lastly, calibration contributes to traceability and standardization within the healthcare sector. The process involves comparing measurements obtained from a medical device against a traceable reference standard, establishing a chain of traceability that ensures consistent measurements across different devices and locations. This standardization facilitates effective communication, collaboration, and data sharing among healthcare providers and institutions, promoting a cohesive healthcare ecosystem [27].

 doi:10.20944/preprints202404.1560.v1

In conclusion, medical device calibration occupies a pivotal position in healthcare, warranting attention due to its role in enabling accurate measurements, ensuring patient safety, maintaining regulatory compliance, supporting quality control initiatives, preserving data integrity, optimizing device longevity, and fostering traceability and standardization. As such, calibration practices are instrumental in delivering effective healthcare and promoting favorable patient outcomes [28].

3.1. Equipment Architecture

The proposed device consists of two elements that can work together or independently. First, it is a force sensor system that can measure and display the applied force. The other is an accurate linear displacement system for simulating various SWM application scenarios. The various components that make up the developed device and their interactions are shown in the diagram in Figure 2. The equipment should be interfaced with a computer to allow the better equipment operation, for the observation of evaluation charts, data persistence, and statistics, among other functionalities. During development, preference was given to standard components already tested and available on the market. Where this was not possible, specific parts were designed from scratch and designed and simulated using 3D modeling software to ensure all project requirements and desired properties were met. Prototypes were then printed with 3D printing technology using PLA (a type of organic biodegradable thermoplastic polymer), tested and improved when necessary. These parts showed to have good mechanical resistance and operational reliability in the desired operation conditions, thus giving them an excellent performance for their purpose.

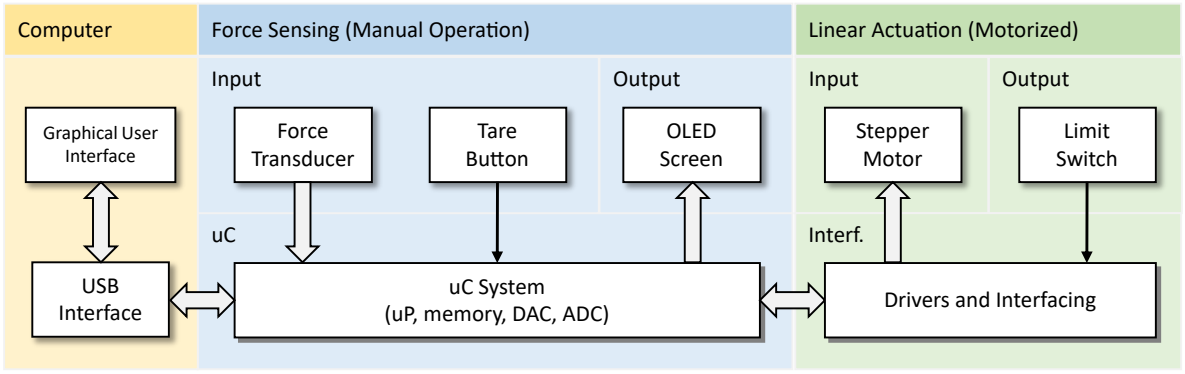

Figure 2. Main equipment components and their interaction (uC - microcontroller, uP - microprocessor, DAC - digital to analog converter, ADC - analog to digital converter, Interf. - interface).

3.2. Force Sensing System

This is a portable element and can be operated alone to carry out measurements with manual application of the monofilament and take measurements, thereby sensing the value of the applied force. However, it can also be coupled with the precision linear displacement system (PLDS) (described next) and work together as a single mechanism in automatic mode. The force sensing system (FSS) (see Figure 3), in summary, is equipped with an OLED screen, a force transducer, a button to carry out the tare measurement, a connector for power input and a USB Mini-B input for communication with a computer. Finally, an electronic controller (composed by microprocessor, memory, and digital converters), based on the IC ATmega328, is responsible for carrying out all the programmed operations and executing the commands that will be sent through a computer application. When in automatic mode, the computer fully controls the equipment, i.e. when the FSS is coupled with the PLDS. The fundamental element consists of a force measurement platform, shaped similar to the anatomy of the plantar region of a human foot, which, in turn, is coupled to the force transducer. The surface of the platform has ethylene-vinyl acetate coating with a texture and hardness chosen to be similar to what is observed with real biological tissues. It will be on this platform that the monofilaments under evaluation will apply their strength, in a movement similar to the technique used in the sensitivity

 doi:10.20944/preprints202404.1560.v1

evaluation of the diabetic foot. Through this measurement process it will be possible to obtain the respective inherent value of the buckling force applied by the SWM.

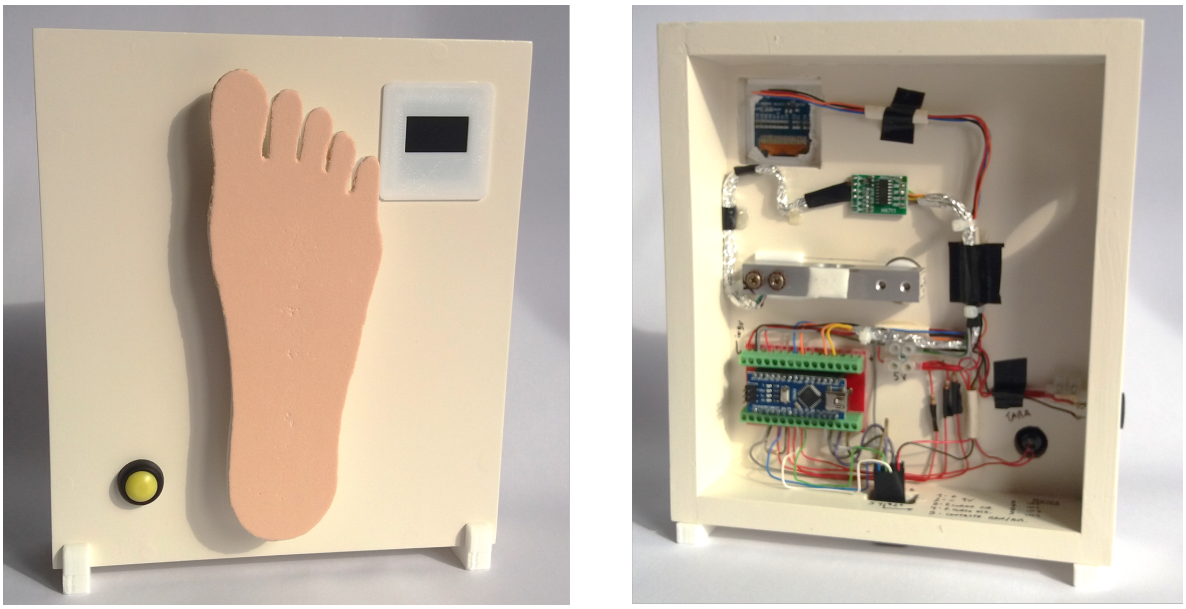

Figure 3. Force sensing system and its measurement platform shaped similar to the plantar region of the foot: external view of the module for manual measurement (left) and inner hardware components (right).

3.3. Precision Linear Displacement System

This PLDS mechanism is responsible for the motorized application of the SWM. Therefore, for this mechanism to operate, it has to be coupled to the force sensing component, since, in turn, this is what contains all the control electronics, computer interfacing (through a dedicated application) and is responsible for measuring the buckling force of the monofilaments that will be subject to metrological verification. PLDS element is comprised of a stepper motor, a v-shaped sliding guide, a trolley with bearings and a fixation support for the SWM. This set of components will carry out the movements to apply the strength of the monofilaments, simulating the technique used by health professionals on the diabetic foot assessment. In Figure 4 the full equipment can be observed in detail. The PLDS, depicted in a lower position, has visible slots for the rods connecting the visible tray with the motorized mechanism, hidden below. The top clamp, mounted on the tray, is used to robustly fixate the SWM, as shown. It allows to adjust pitch and yaw incidence angles, creating the possibility for different testing conditions. Finally, in the rightmost area the FSS platform (already described) can be observed, which in this case is operating integrated with the PLDS.

The hidden stepper motor is responsible for moving a reinforced rubber belt, connected to a guided chariot. With this setup it is capable of performing precise linear movements. It basically consists of a movement of the visible tray that follows with the SWM attached and simulates the technique of applying the monofilament to the patient's foot. The monofilament is then moved and comes into contact with the measurement platform where the applied force is measured, as this platform is coupled to the force transducer. These displacement movements of the monofilament fixation support are provided by the gantry and v-shaped sliding guide. The motion is supported by a transmission belt that is engaged in a pulley coupled to the stepper motor shaft, assuring the desired precision. The displacement is electronically controlled and can be performed in linear and continuous movements, forwards and backwards, with end-of-course control or the number of steps taken.

 doi:10.20944/preprints202404.1560.v1

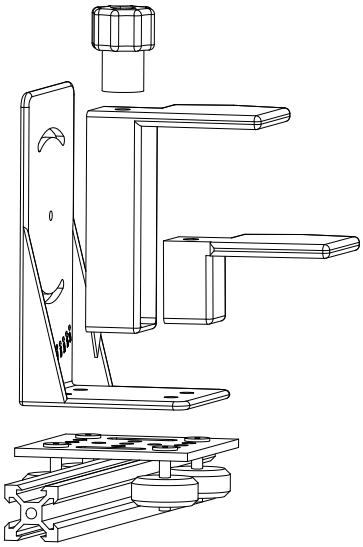

(a) CAD drawing of the PLDS system with expanded components.

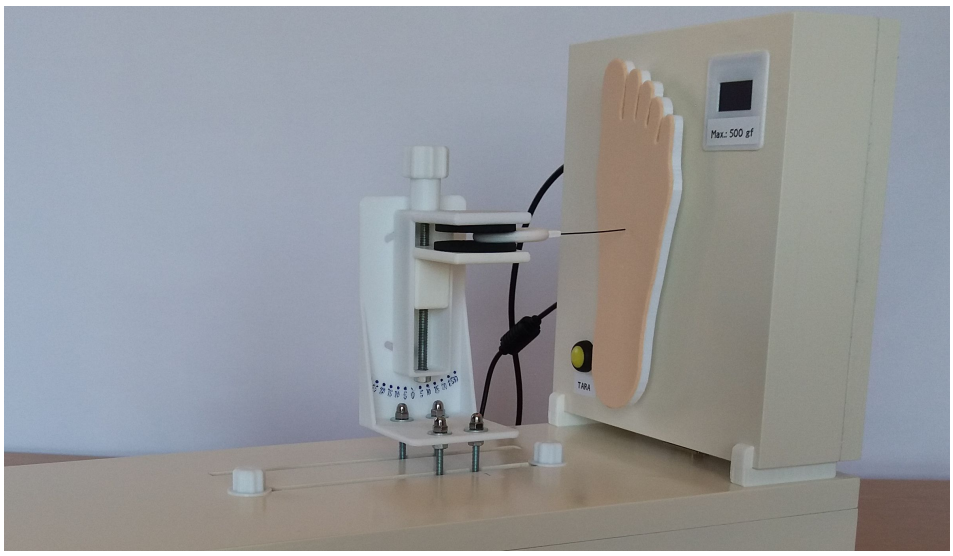

(b) Photographic image of the implementation of the PLDS and FSS systems.

Figure 4. Proposed equipment, with a detailed view of the precision linear displacement system integrated with the force sensing system platform.

3.4. Equipment Technical Specifications

Since the proposed equipment is intended to serve as a measurement system, it is important to consider the inherent accuracy and precision characteristics of force transducers, the components that convert physical quantities into corresponding electrical signals. To ensure that the equipment transmits quality estimates of the applied forces, it was subjected to a calibration process using a compression machine (MecMesin Multitest 10-i) with a load cell. This compression machine is approved to carry out calibration tests and its main characteristics are detailed in Table 2. This step allowed adjustments to the proposed equipment's measurement algorithm to ensure precise and accurate measurements in a range of 0.1 gf to 500 gf.

 doi:10.20944/preprints202404.1560.v1

Table 2. Technical specifications of the compression testing machine - MecMesin Multitest 10-i.

Specification	Value/Description
Load cell ref.	ILC 10N
Range (N)	0 to 10
Resolution (N)	$>$ 0.0001 (1:6500)
Precision (N)	$\pm$ 0.01 (0.1% fs)
Acquisition rate (Hz)	10
Displacement velocity ($mm.s^{-1}$)	0.08 (**a**)

(**a**) Velocity can be controlled.

Although the developed equipment has the capacity to carry out accurate measurements in a wider measurement range, for safety reasons the force transducer was limited to 500 gf of maximum admissible load, which is within the expected SWM test values. This step ensures the integrity of the equipment and makes it possible to adapt it to other assessments with monofilaments of a caliber greater than 10 gf (there are calibers of up to 300 gf on the market, more used to assess deep sensitivity). If 500 gf are exceeded, all system operation is aborted and an error message appears on the screen, instructing the user to remove the load and reset the equipment. The internal resolution of the sensing stage is high (the integrated analog to digital convert offers a 10-bit resolution with $\pm$ 2LSB accuracy), allowing to obtain a high number of decimal places. During development, a balance must be found between information accuracy and usefulness. Hence, it should be noted that, although the measuring equipment is capable of operating with a higher resolution, the measured values in the range 0 gf to 99.9 gf are presented rounded to a single decimal place. In the hundreds range, from 100 gf to 500 gf, measured values are rounded to the nearest unit. This procedure guarantees a balanced rounding and speeds up the comparison of the values obtained in the measurements with the values declared by the monofilament manufacturers. The same approach can be used to evaluate other monofilament calibers.

The PLDS is intended to perform high precision movements. For this, a stepper motor, powered by a ULN2003A based electronic driver, and a toothed belt drive are used. This setup is capable of making minimum increments of 0.08 mm in the displacement steps, this at the time of a given measurement. Still regarding the characteristics of the linear displacement component, a total space of approximately 140 mm can be covered, enough to manipulate the various models of monofilaments available on the market. Table 3 shows the most relevant technical specifications of the proposed equipment, where measurement range, resolution, precision and accuracy were obtained through the calibration process with the MecMesin Multitest machine.

Table 3. Detailed equipment specifications.

Specification	Value/Description
Range (gf)	(**a**) 0.1 to 99.9 and (**b**) 100 to 500
Resolution (gf)	(**a**) 0.1 and (**b**) 1
Precision (gf)	(**a**) $\pm$ 0.03 and (**b**) $\pm$ 0.25
Accuracy (%)	(**a**) $\pm$ 0.36 and (**b**) $\pm$ 0.68
Displacement resolution (mm)	0.08
Power supply (V DC)	9
Computer interface	USB mini-B connector; Specific Windows app
Modes	Linear by limit switch and by number of steps

(**a**) Rounds the measurement value to a single decimal place; (**b**) Rounds the measurement value to unity.

When the equipment is operated in automatic mode, it is necessary to connect it to a computer through a USB Mini-B communication cable. This communication allows, through a specific computer application, developed for this purpose, to operate the equipment and receive all the information

 doi:10.20944/preprints202404.1560.v1

relating to each monofilament evaluation. As for the energy source of this equipment, it is powered by an external source of 9 V DC.

4. Methods, Results and Discussion

Analyzing the literature, there is still uncertainty about the effective accuracy and precision of monofilaments in their use to test the loss of sensitivity in the diabetic foot. Therefore, the methodology applied in the present study was organized with the aim of obtaining a concrete answer, performing a rigorous metrological verification of fourteen SWM of 10 gf (from different manufacturers) most used by the medical community in general. For this verification, equipment capable of simulating the conventional procedure used by health professionals was created (previously described). This procedure registers the behavior of the nylon filament until it deforms with the recommended curvature, at which point the force declared by its manufacturer will have been applied. The equipment will also be able to perform fatigue tests to assess performance after several repetitions.

In the following subsections, a set of different scenarios that were used to explore the proposed calibration equipment, as well as the analytical model of the monofilament, will be presented.

4.1. Equipment Validation

To evaluate the measurement performance of the proposed equipment, it was submitted to a series of validation procedures through controlled tests with a MecMesin compression machine. This machine, with a valid calibration certificate from a national metrological institution, is able to produce a controlled pre-determined force with a precision of $\pm$ 0.01 N. The MecMesin can also provide information about the force that was produced with a resolution of $\pm$ 0.0001 N ((by other words the actuation control system is not able to achieve the same resolution as the measuring system). The test protocol consisted of compressing the FSS of the proposed equipment into several measurement points plus a random increase of $\leq$ 25%, in rounds of thirty measurements for each. The mean compressive force values of each set and the respective standard deviation obtained by the MecMesin machine and the proposed equipment were recorded. The obtained results can be observed in Table 4. It should be noted that the standard deviation (SD) values indicated by the MecMesin machine were deliberately provoked to verify whether the FSS equipment followed the same behavior.

Table 4. Mean force and related standard deviation ($\pm$ SD) from the MecMesin and FSS equipments. The MecMesin row shows the mean and standard deviation the generated forces and the FSS row shows the measured forces related statistics. For each reference point, a round of thirty measures were obtained, with a room temperature of 20 ºC.

Reference Point	6 gf	10 gf	15 gf	20 gf	50 gf	300 gf
MecMesin	6.4 $\pm$ 0.5	11.3 $\pm$ 0.1	16.7 $\pm$ 0.1	22.2 $\pm$ 0.6	80.0 $\pm$ 3.7	344.3 $\pm$ 26.2
FSS	6.4 $\pm$ 0.5	11.3 $\pm$ 0.1	16.7 $\pm$ 0.1	22.3 $\pm$ 0.6	80.0 $\pm$ 3.9	345.6 $\pm$ 26.3

In addition, the obtained results were plotted using Bland-Altman plots [29]. This type of representation provides a valuable visual representation to observe the agreement between two measuring instruments. It allows for a quick assessment of comparability or discrepancies between the instruments. The plot displays the mean difference between the measurements obtained from the two instruments as a horizontal line, which, if close to zero, indicates little to no systematic bias. Moreover, the limits of agreement (corresponding to $\pm$1.96 standard deviations, or a 95% confidence interval), represented by two horizontal dashed lines above and below the mean difference line, offer insight into the range within which most of the differences lie. Any deviation from a consistent distribution of points around the mean difference line may suggest proportional bias, wherein differences vary with measurement magnitude. Outliers in the plot are easily identifiable and can highlight potential measurement errors or instances where one instrument performs exceptionally well or poorly.

 doi:10.20944/preprints202404.1560.v1

In Figure 5 the very good performance of the proposed equipment can be observed, either in the 10 gf monofilament operation range (Figure 5a) but also near its operational limits (Figure 5b). Near the 350 gf reference point, it can be observed that the values differences are higher and always positive. This is due to the combination of numerical rounding in the MecMesim system and also in the proposed system. This aspect does not have relevance for the specific purposes of this study, whose operational range is near 10 gf, where excellent metrological properties were observed.

The obtained results showed that the FSS equipment presented very precise and consistent measurements, which is a positive indication of the performance of the proposed equipment. The comparison of the values obtained by the FSS equipment with the values measured by the MecMesin machine allowed to verify the reliability of the measurements carried out by the FSS. The very similar standard deviation values between the two devices indicate that the FSS measurements are consistent and demonstrate that the proposed equipment has a good repeatability capability in its measurements. It should be noted that the mean relative error, calculated on all tests of the various measurement ranges, was approximately 0.28%. These results also show that the FSS equipment is able to perform the SWM buckling force measurement tests with accurate and reliable results. If the analysis interval is the force range that is often used for diabetic foot related procedures, the proposed system can achieve the highest measuring performance.

 doi:10.20944/preprints202404.1560.v1

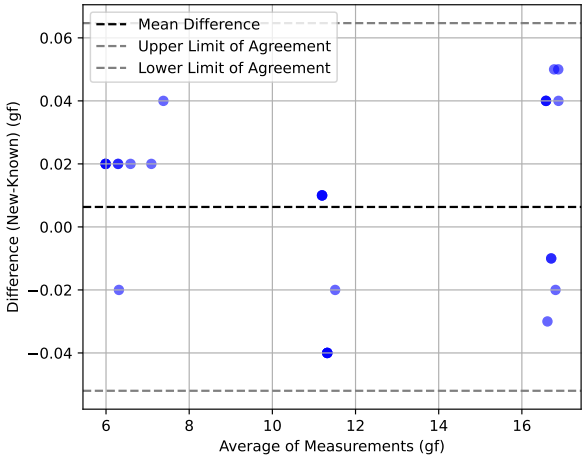

(a) For reference forces near the 10 gf monofilament operation range.

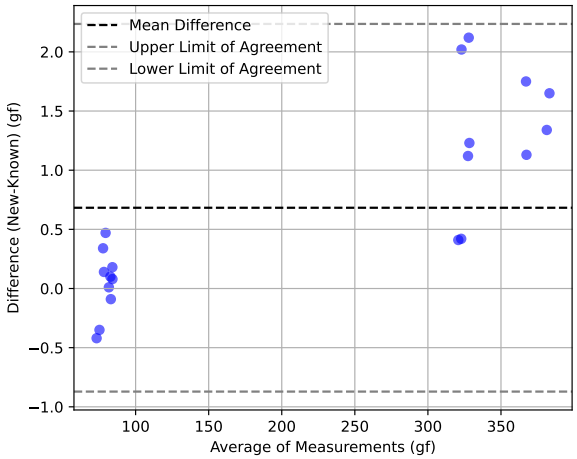

(b) For reference forces near the operational range limit of the proposed equipment.

Figure 5. Bland-Altman plots comparing a reference equipment (MecMesin) and the proposed equipment (FSS).

4.2. Monofilament Compression

After ensuring optimal accuracy and consistency of the calibration equipment, a set of tests was performed with monofilaments devices used for the plantar sensitivity test. Fourteen monofilaments with a force threshold of 10 gf were carefully chosen from diverse manufacturers. All the devices were in new condition and none had information besides the critical force. All tests were conducted at a stable room temperature of 20 °C to minimize environmental influences on the results. The monofilament, starting from a reference position, was longitudinally displaced towards the FSS, by 10 mm (necessary displacement to make the buckling curvature recommended), applying force in a perpendicular direction in relation to the platform. This setup mirrored real-life scenarios and facilitated precise plantar sensitivity evaluations. To assess the impact of different monofilament progression speeds on plantar sensitivity, two values were used: 4 $mm.s^{-1}$ and 8 $mm.s^{-1}$. Again, these speed choices were chosen with the purpose of mimicking the human-made procedure. It should be noted that the tests with different speeds were performed with a difference of 24 hours between them to minimize potential effects of memory or fatigue on the monofilament.

 doi:10.20944/preprints202404.1560.v1

Figure 6 illustrates the force/displacement charts obtained from the experimental data. Upon compression initiation, two distinct regimes become apparent: a linear regime before reaching the critical force F_c, and a buckling regime that follows thereafter. The force contours of the tested devices can be categorized into two groups. The first group exhibits an incremental force rise up to its critical value, maintaining relative stability throughout the entire displacement range. In contrast, the second group demonstrates an overshooting phenomenon, with the critical force slowly decaying during buckling. This behavior may arise from the utilization of monofilament material, which offers superior resistance to compression compared to deflection. By comparing the two charts, it can be observed that, when the displacement speed is higher, this effect is less visible. Looking at the final values, it can be observed that all monofilaments provided a force that is different from the expected 10 gf and, many of them, exerted a force that is twice the expected value. A smaller diversity of behaviours for the 8 $mm.s^{-1}$ scenario can also be observed.

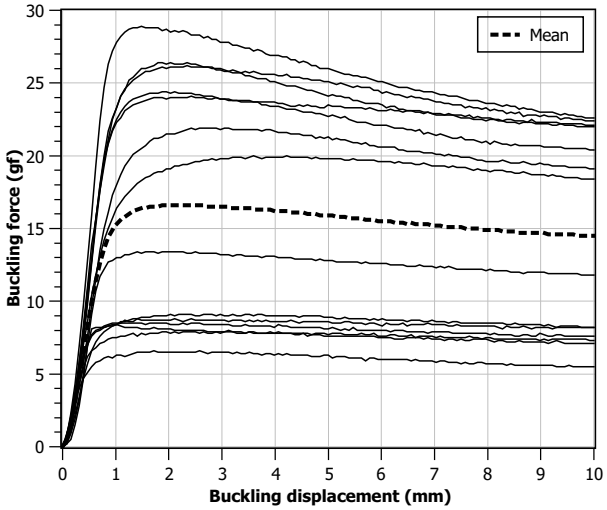

(a) Progression speed of 4 $mm.s^{-1}$.

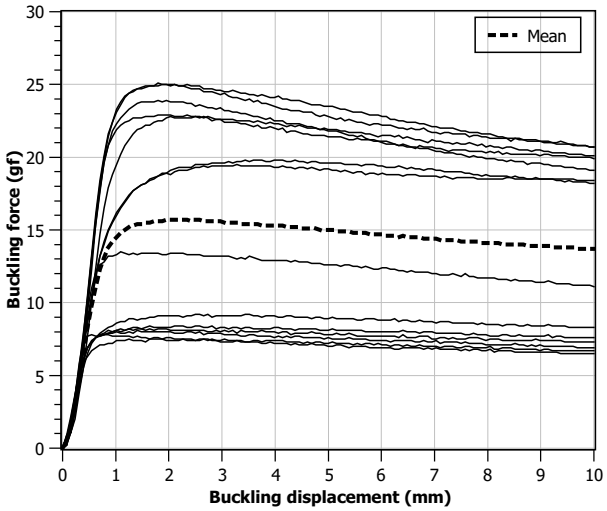

(b) Progression speed of 8 $mm.s^{-1}$.

Figure 6. Force values measured with the FSS system as a function of monofilament displacement. Each line represents one monofilament. The dashed line is calculated as the mean value of the other lines.

 doi:10.20944/preprints202404.1560.v1

4.3. Monofilament Stress Tests

Utilizing a monofilament in isolation for testing purposes may not fully represent the real-world conditions in which the device is intended to be used. To better simulate actual usage scenarios, it was decided to investigate the behavior of each of the fourteen monofilaments through a sequence of 20 consecutive compression cycles, with a time interval of 3 seconds between consecutive compressions. The experiments were conducted at a room temperature of 20 °C and at two distinct displacement speeds, as in the previous test. Again, tests with different speeds were performed with a difference of 24 hours between them to minimize possible effects of memory or fatigue on the monofilament.

Figure 7 presents charts for the critical force measurements obtained for each monofilament across the 20 cycles. It can be observed that all monofilaments have a higher critical force in the first compression trial that starts to decay with repeated compressions. On average, this effect is slower and smaller when a lower displacement speed is used. For the higher displacement speed, most monofilaments reach a force plateau after the second compression. It can also be observed that, in both scenarios, the average value is above the expected 10 gf, being around 15 gf for the 4 $mm.s^{-1}$ and around 13 gf for the 8 $mm.s^{-1}$ case. In the faster displacement scenario, it can be observed that two monofilaments do not provide a contour patterns compatible with all the others. This may point to geometrical defects during manufacturing or non homogeneous material distribution.

 doi:10.20944/preprints202404.1560.v1

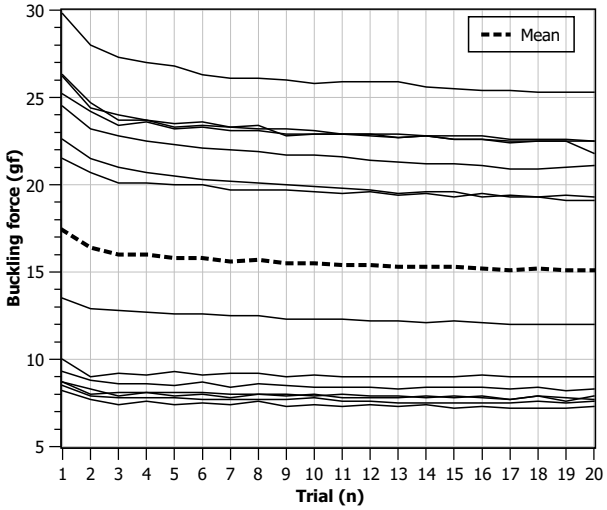

(a) Progression speed of 4 $mm.s^{-1}$.

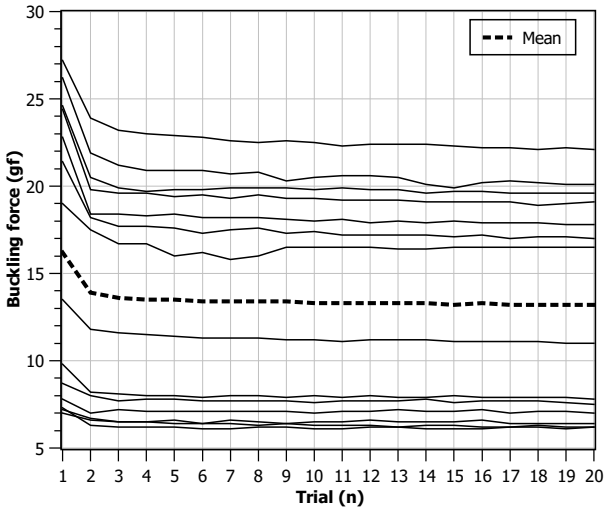

(b) Progression speed of 8 $mm.s^{-1}$.

Figure 7. Critical force values during 20 trials. Each line represents one monofilament. The series mean value is calculated and represented as a dashed line.

Figure 8 shows the charts for the critical force values for each monofilament independently. Two groups (1 to 6 and 7 to 12), showing to share similar behaviour during the experiments, can clearly be observed. In general, it can be observed the monofilament device can be reliable for repeated usage but a high precision manufacturing process is mandatory.

 doi:10.20944/preprints202404.1560.v1

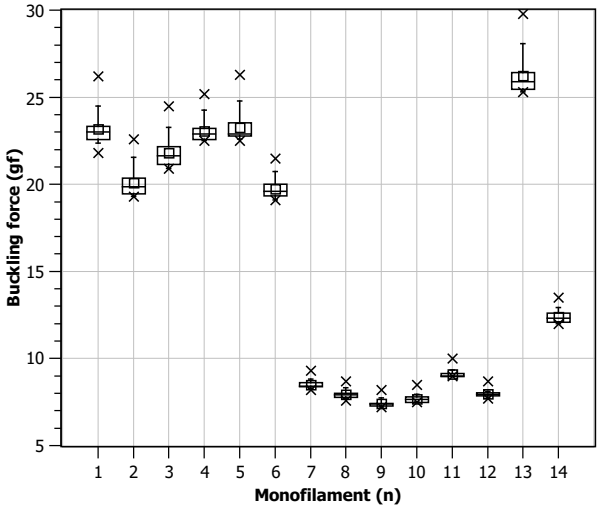

(a) Progression speed of 4 $mm.s^{-1}$.

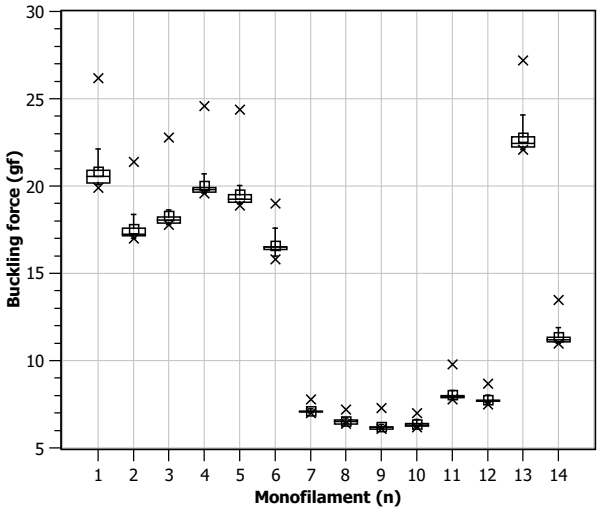

(b) Progression speed of 8 $mm.s^{-1}$.

Figure 8. Critical force values after 20 trials.

The above presented experiments and the reported results provide valuable insights into the monofilament's performance under repeated compression, reflecting its ability to withstand continuous usage and offering a more comprehensive understanding of its behavior in practical applications, since these instruments, after being disinfected, can be used several times a day in several patients.

4.4. Theoretical Value of Critical Force

From equation (4), substituting for the values obtained by measuring a specimen of 10 gf monofilament under study, it can be written:

$d = 0.61\ mm = 0.00061\ m$

$$I = \frac{\pi \cdot (0.00061)^4}{64}$$

To calculate the effective length ($L_{\text{effective}}$), the boundary conditions must be considered. For a clamped-free condition, the effective length is considered to be 0.7 times the actual length. Therefore:

$L = 38\ mm = 0.038\ m$

 doi:10.20944/preprints202404.1560.v1

$$L_{\text{effective}} = 0.7 \cdot 0.038 = 0.02660\ m$$

Now, the Young's modulus (E) of the nylon material must be introduced. For the purpose of this example, a typical value for nylon was assumed, being approximately 2 GPa (2×10^9 Pa). All the values into Euler's buckling equation can be replaced (3):

$$F_{\text{critical}} = \frac{\pi^2 \cdot (2 \times 10^9) \cdot \left(\frac{\pi \cdot 0.00061^4}{64}\right)}{0.02660^2}$$

Simplifying the equation, it is obtained:

$$F_{\text{critical}} \approx \pi^2 \cdot (2 \times 10^9) \cdot \left(\frac{\pi \cdot 0.00061^4}{64}\right) \cdot \left(\frac{1}{0.02660^2}\right) \approx 0.18961\ N$$

The resulting value will be in units of force, such as newtons (N). To make a direct comparison with the target values of the monofilaments possible, which can be converted to the mass unit:

$$m = \frac{F}{a} = \frac{0.18961}{9.80665} = 0.01933\ kg = 19.33\ g$$

Therefore, this monofilament has a critical buckling force of approximately 19.33 gf, well above the 10 gf declared by the manufacturer, but compatible with some of the obtained test results, as in Figure 6. However it should be noted that these calculations assume linear elastic behavior and neglect any other factors that may affect the buckling behavior, such as imperfections or other deformation complexities. Additionally, the actual buckling behavior of a nylon filament may also depend on other factors like temperature, moisture and manufacturing tolerances, as mentioned.

4.5. Material and Geometry Variations

Using the measures obtained during the monofilaments calibration tests (in section 4.2), the materials' Young's modulus was calculated for each device, as seen in Table 5. The average value for the Young's modulus is 2.74 Gpa, which is within the expected range of values for a nylon polymer. These values were then used to calculate how the monofilament behaves when there is slippage of the free extremity, shown in the rightmost column. The effective length L_e of the monofilament is a quadratic parameter in equation 3, showing that inadequate friction conditions between the monofilament and the skin surface will have a very significant impact on the result and quality of the SWM test.

Table 5. Monofilament properties for four distinct devices. The materials' Young's moduli E was calculated from previously obtained geometrical dimensions, length L and diameter d, and critical force measures F_c, considering clamped-pinned boundary conditions ($k = 0.7$, corresponding to the device calibration procedure setup conditions). Using E, a new critical force was calculated considering clamped-sliding boundary conditions ($k = 2.0$).

#	d (mm)	L (mm)	E (GPa)	I (m^4)	F_c (k = 0.7) (gf)	F_c (k = 2.0) (gf)
1	0.61	38	**2.99**	6.797E-15	*28.91*	**3.54**
2	0.46	41	**3.65**	2.198E-15	*9.80*	**1.20**
3	0.71	38	**1.68**	12.474E-15	*29.81*	**3.65**
4	0.52	38	**2.65**	3.589E-15	*13.50*	**1.65**

From equation 3 it can be observed that, while Young's modulus appears as linear coefficient, the length is squared, being more relevant for the force's final value. In equation 4, a linear factor in equation 3, it can be observed that d has a fourth order exponent, making small variations in the variable to have a high impact on the result.

 doi:10.20944/preprints202404.1560.v1

Figure 9 shows the critical force as a function of monofilament length and diameter, for two distinct Young's modulus. The effect of increased length and reduced diameter (for example considering a 10% manufacturing tolerance) can lead to a severe difference in the critical force. By observing the contour lines orientation, the importance of diameter variations can be identified as highly relevant for the devices' performance (as expressed in equation 4). A correct choice of the material is also an important factor to consider for manufacturing purposes since a low value for the Young's modulus allows a higher dimensional tolerance.

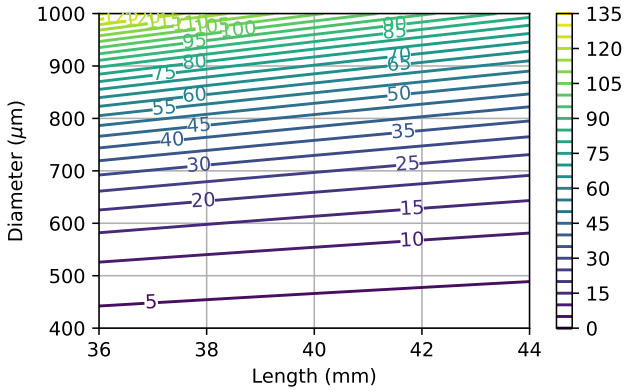

(a) $E = 1.68\ GPa$.

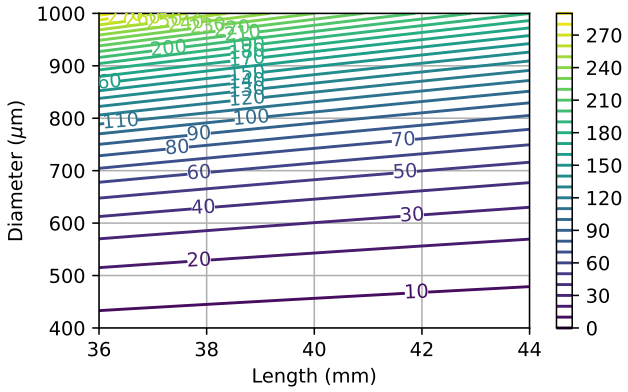

(b) $E = 3.65\ GPa$.

Figure 9. Critical force as a function of the monofilament length L and diameter d. Values are in gf. The Young's modulus correspond to the minimum and maximum values that were estimated during calibration tests.

Deflection due to the monofilament weight can have a major impact on the device performance since, as seen in Figure 6, there are two distinct regimes during compression, mediated by the occurrence of the critical buckling force. When the monofilament has a higher length and smaller diameter, assuming equal material properties, then the deflection will be higher and the transition between the two observed regimes does not present an overshoot.

In the center of Table 6 (in bold typeface) the deflection value δ is shown, due to its own weight, for the longest ($L = 41\ mm$) and thinnest ($d = 0.46\ mm$) monofilament of the experimental test set. For this case, the relative deflection in relation to its diameter $\delta(\%d)$ was 17.8%. This monofilament (and others in the test set with similar properties) shows no overshoot in the force/displacement contours of Figure 6 (the monofilaments group whose curves are shown lower in the chart). For the shortest ($L = 38\ mm$) and thickest ($d = 0.71\ mm$) monofilament (not shown in Table 6) the deflection was $\delta = 55\ \mu m$, correspoding to 7.8% of its diameter.

 doi:10.20944/preprints202404.1560.v1

Table 6. Deflection of the devices' free extremity due to its own weight, considering 10% variations (increase or decrease) in the monofilament length L and diameter d. Absolute values δ are in μm. Relative deflection $\delta(\%)$ have the 10 gf monofilament deflection (center, bold typeface) as reference. Relative deflection $\delta(\%d)$ have the diameter of each monofilament as reference. The reference monofilament had length $L = 41\ mm$, diameter $d = 0.46\ mm$, Young's modulus $E = 3.65\ GPa$, and density 1100 $Kg.m^{-3}$.

$d \backslash L$	$L(-10\%)$			$L(0\%)$			$L(+10\%)$		
	$\delta(\mu m)$	δ (%)	$\delta(\%d)$	$\delta(\mu m)$	δ (%)	$\delta(\%d)$	$\delta(\mu m)$	δ (%)	$\delta(\%d)$
$d(-10\%)$	66.26	-19%	16.0%	100.99	23%	24.4%	147.87	81%	35.7%
$d(0\%)$	53.67	-34%	11.7%	**81.81**	**0%**	**17.8%**	119.77	46%	26.0%
$d(+10\%)$	44.36	-46%	8.8%	67.61	-17%	13.4%	98.98	21%	19.6%

From equations 4 and 7 it can be seen that both diameter d and length L have a high impact on the monofilament deflection behaviour, as can be observed in the variations presented in Table 6. The highest relative deflection $\delta(\%)$ was obtained for 10% increase in the monofilament length and a 10% decrease in its diameter, leading to a deflection increase of 81%.

5. Conclusions

In this article, a novel equipment designed for the automatic metrological evaluation of SW monofilaments was introduced, providing a valuable tool for both objective assessment and training of health professionals in the SWM test procedure. The present study demonstrates the system's capability to automatically evaluate monofilaments, yielding detailed and precise displacement vs. force contours that characterize the behavior of each individual device.

Notably, the presented findings reveal that the forces applied by the monofilaments may deviate from the manufacturers' specifications, highlighting the importance of accurate calibration and testing parameters for reliable clinical assessments. Understanding these discrepancies contributes to the refinement of neurological diagnosis and rehabilitation strategies, enabling more effective treatment decisions.

In addition to presenting a new equipment for the automatic metrological evaluation of SW monofilaments, this study encompasses the development of analytical models to comprehend the influence of each variable on the critical buckling force during monofilament compression. These analytical models serve as valuable tools to investigate and dissect the complex behavior of monofilaments under compression, allowing us to gain deeper insights into the factors that significantly impact the critical buckling force. By employing these analytical models, it was possible to discern the interplay between various parameters, shedding light on their individual contributions to the overall behavior of the monofilaments during the compression process.

The combination of experimental results and analytical modeling provides a robust framework for comprehending the mechanical behavior of SW monofilaments and paves the way for future research and improvements in plantar sensitivity evaluation. With this knowledge, health professionals can make more informed decisions when interpreting results and devising adequate follow-up routines and treatment plans for patients based on accurate and precise data.

In conclusion, this work lays the foundation for a more robust and precise evaluation and usage of SW monofilaments, ultimately aiding in the enhancement of clinical practices and decisions.

Funding: This research was developed under a PhD grant (UI/BD/151285/2021) awarded to PCM and funded by the Portuguese Foundation for Science and Technology (FCT, Portugal). It was also partially supported by FCT-UIDB/04730/2020 and FCT-UIDB/50014/2020 projects.

Data Availability Statement: Data are available on request to the corresponding author.

Acknowledgments: Special thanks to the Biomechanics Laboratory of the Institute of Science and Innovation in Mechanical and Industrial Engineering (INEGI, Porto, Portugal) for granting access to the load cell compression machine.

Conflicts of Interest: The authors declare no conflict of interest.

 doi:10.20944/preprints202404.1560.v1

References

1. Bus, S.A.; Armstrong, D.G.; Gooday, C.; Jarl, G.; Caravaggi, C.; Viswanathan, V.; Lazzarini, P.A.; Lavery, L.A.; Monteiro-Soares, M.; Rasmussen, A.; Raspovic, A.; Sacco, I.C.; van Netten, J.J.; Armstrong, D.G.; Gooday, C.; Jarl, G.; Caravaggi, C.; Viswanathan, V.; Lazzarini, P.A. Guidelines on offloading foot ulcers in persons with diabetes (IWGDF 2019 update). *Diabetes/Metabolism Research and Reviews* **2020**, *36*, 1–18. doi:10.1002/dmrr.3274.
2. Bus, S.A.; Lavery, L.A.; Monteiro-Soares, M.; Rasmussen, A.; Raspovic, A.; Sacco, I.C.; van Netten, J.J. Guidelines on the prevention of foot ulcers in persons with diabetes (IWGDF 2019 update). *Diabetes/Metabolism Research and Reviews* **2020**, *36*, 1–18. doi:10.1002/dmrr.3269.
3. Olaiya, M.T.; Hanson, R.L.; Kavena, K.G.; Sinha, M.; Clary, D.; Horton, M.B.; Nelson, R.G.; Knowler, W.C. Use of graded Semmes Weinstein monofilament testing for ascertaining peripheral neuropathy in people with and without diabetes. *Diabetes Research and Clinical Practice* **2019**, *151*, 1–10. doi:10.1016/j.diabres.2019.03.029.
4. Schaper, N.C.; van Netten, J.J.; Apelqvist, J.; Bus, S.A.; Hinchliffe, R.J.; Lipsky, B.A. *IWGDF Guidelines on the prevention and management of diabetic foot disease*; The International Working Group on the Diabetic Foot, 2019.
5. Costa, T.; Coelho, L.; Silva, M.F. Automatic Segmentation of Monofilament Testing Sites in Plantar Images for Diabetic Foot Management. *Bioengineering* **2022**, *9*, 86. doi:10.3390/bioengineering9030086.
6. Costa, T.; Coelho, L.; Silva, M.F. Integrating Computer Vision, Robotics, and Artificial Intelligence for Healthcare: An Application Case for Diabetic Foot Management. In *Exploring the Convergence of Computer and Medical Science Through Cloud Healthcare*; Coelho, L.; Queiros, R., Eds.; IGI Global, 2023; p. 29. doi:10.4018/978-1-6684-5260-8.ch007.
7. Wang, F.; Zhang, J.; Yu, J.; Liu, S.; Zhang, R.; Ma, X.; Yang, Y.; Wang, P. Diagnostic Accuracy of Monofilament Tests for Detecting Diabetic Peripheral Neuropathy : A Systematic Review and Meta-Analysis. *Journal of Diabetes Research* **2017**, *2017*. doi:10.1155/2017/8787261.
8. Martins, P.; Coelho, L. Evaluation of the Semmes-Weinstein Monofilament on the diabetic foot assessment. In *Advances and Current Trends in Biomechanics*; Belinha, J.; Campos, J.C.R.; Fonseca, E.; Silva, M.H.F.; Marques, M.A.; Costa, M.F.G.; Oliveira, S., Eds.; CRC Press: Porto, 2021. doi:10.1201/9781003217152.
9. Chikai, M.; Ino, S. Buckling Force Variability of Semmes-Weinstein Monofilaments in Successive Use Determined by Manual and Automated Operation. *Sensors MDPI* **2019**, *19*. doi:10.3390/s19040803.
10. Lavery, L.A.; Lavery, D.E.; Lavery, D.C.; Lafontaine, J.; Bharara, M.; Najafi, B. Accuracy and durability of Semmes-Weinstein monofilaments: What is the useful service life? *Diabetes Research and Clinical Practice* **2012**, *97*, 399–404. doi:10.1016/j.diabres.2012.04.006.
11. Young, M. A perfect 10? Why the accuracy of your monofilament matters. *Diabetes and Primary Care* **2009**, *11*, 40–43.
12. Haloua, M.H.; Sierevelt, I.; Theuvenet, W.J. Semmes-Weinstein Monofilaments: Influence of Temperature, Humidity, and Age. *American Society for Surgery of the Hand* **2011**, *36*, 1191–1196. doi:10.1016/j.jhsa.2011.04.009.
13. Campo, E.A. 2 - Mechanical Properties of Polymeric Materials. In *Selection of Polymeric Materials*; Campo, E.A., Ed.; Plastics Design Library, William Andrew Publishing: Norwich, NY, 2008; pp. 41–101. doi:10.1016/B978-081551551-7.50004-8.
14. Schaper, N.C.; van Netten, J.J.; Apelqvist, J.; Bus, S.A.; Hinchliffe, R.J.; Lipsky, B.A. Practical Guidelines on the prevention and management of diabetic foot disease (IWGDF 2019 update). *Diabetes/Metabolism Research and Reviews* **2020**, *36*, 1–10. doi:10.1002/dmrr.3266.
15. Martins, P.; Coelho, L. A New Equipment for Automatic Calibration of the Semmes-Weinstein Monofilament. 32nd Flexible Automation and Intelligent Manufacturing International Conference (FAIM'23); Springer International Publishing: Porto, 2023; Lecture Notes in Mechanical Engineering. doi:10.1007/978-3-031-38241-3_21.
16. Ugo Basile. Von Frey Hairs, Semmes-Weinstein set of monofilaments. Available online: https://ugobasile.com/products/catalogue/pain-and-inflammation/item/52-37450-275-von-frey-hairs (accessed on 11 July 2023), 2023.
17. Medical Monofilament Manufacturing. The most effective medical device for diabetic foot screening from the only manufacturer with FDA 510(k) clearance. Available online: https://medicalmonofilament.com (accessed on 11 July 2023), 2023.

 doi:10.20944/preprints202404.1560.v1

18. van Netten, J.J.; Raspovic, A.; Lavery, L.A.; Monteiro-Soares, M.; Rasmussen, A.; Sacco, I.C.; Bus, S.A. Prevention of foot ulcers in the at-risk patient with diabetes: a systematic review. *Diabetes/Metabolism Research and Reviews* **2020**, *36*, 1–22. doi:10.1002/dmrr.3270.
19. Zhou, S.M.; Tashiro, K.; Ii, T. Moisture Effect on Structure and Mechanical Property of Nylon 6 as Studied by the Time-Resolved and Simultaneous Measurements of FT-IR and Dynamic Viscoelasticity under the Controlled Humidity at Constant Scanning Rate. *Polymer Journal* **2001**, *33*, 344–355. doi:10.1295/polymj.33.344.
20. Zuo, X.; Zhang, J.; Tang, W.; Li, Y.; Li, H. Buckling behavior of steel and steel–composite cylinders under external pressure. *Thin-Walled Structures* **2022**, *181*, 110011. doi:10.1016/J.TWS.2022.110011.
21. Hutchinson, J.W.; Budiansky, B. Dynamic buckling estimates. *AIAA Journal* **2012**, *4*, 525–530. doi:10.2514/3.3468.
22. Ly, H.B.; Desceliers, C.; Le, L.M.; Le, T.T.; Pham, B.T.; Nguyen-Ngoc, L.; Doan, V.T.; Le, M. Quantification of Uncertainties on the Critical Buckling Load of Columns under Axial Compression with Uncertain Random Materials. *Materials (Basel, Switzerland)* **2019**, *12*, 1828. doi:10.3390/MA12111828.
23. Gere, J.M.; Goodno, B.J. *Mechanics of materials*; Cengage Learning, 2017.
24. Guzzo, D.; Carvalho, M.M.; Balkenende, R.; Mascarenhas, J. Circular business models in the medical device industry: paths towards sustainable healthcare. *Resources, Conservation and Recycling* **2020**, *160*, 104904. doi:10.1016/J.RESCONREC.2020.104904.
25. Veselov, V.; Roytman, H.; Alquier, L. Medical device regulations for process validation: review of FDA, GHTF, and GAMP requirements. *Journal of Validation technology* **2012**, *18*, 82.
26. Badnjevic, A. Evidence-based maintenance of medical devices: Current shortage and pathway towards solution. *Technology and health care : official journal of the European Society for Engineering and Medicine* **2023**, *31*, 293–305. doi:10.3233/THC-229005.
27. Romanchikova, M.; Thomas, S.A.; Dexter, A.; Shaw, M.; Partarrieau, I.; Smith, N.; Venton, J.; Adeogun, M.; Brettle, D.; Turpin, R.J. The need for measurement science in digital pathology. *Journal of pathology informatics* **2022**, *13*, 100157. doi:10.1016/J.JPI.2022.100157.
28. Rajesh.; Gajjala, S.; Agrawal, V.V.; Aswal, D.K. Biomedical Metrology: Role in Nation's Healthcare Sector. *Metrology for Inclusive Growth of India* **2020**, pp. 731–766. doi:10.1007/978-981-15-8872-3_15.
29. Özgür Doğan, N. Bland-Altman analysis: A paradigm to understand correlation and agreement. *Turkish Journal of Emergency Medicine* **2018**, *18*, 139–141. doi:https://doi.org/10.1016/j.tjem.2018.09.001.